

## Measurement of the rare decay $K^\pm \rightarrow \pi^\pm \gamma\gamma$

Plamen PETROV\* for the NA48/2 and NA62 Collaborations†

Centre for Cosmology, Particle Physics and Phenomenology (CP3)

Université catholique de Louvain

2, Chemin du Cyclotron

B-1348 Louvain-la-Neuve

Belgium

E-mail: [plpetrov@cern.ch](mailto:plpetrov@cern.ch)

The recently published measurements of the  $K^\pm \rightarrow \pi^\pm \gamma\gamma$  decay with minimum bias data samples collected by the NA48/2 and NA62 experiments are discussed. The results include a model-independent decay rate measurement and fits to Chiral Perturbation Theory (ChPT) description. The model-independent branching ratio in the kinematic range  $z = (m_{\gamma\gamma}/m_K)^2 > 0.2$ , obtained by combining the NA48/2 and NA62 results, is  $B_{\text{MI}} = (0.965 \pm 0.63) \times 10^{-6}$ . The combined branching ratio in the full kinematic range assuming a ChPT description is  $B_{\text{ChPT}} = (1.003 \pm 0.056) \times 10^{-6}$ . The uncertainties are dominated by the statistical errors. The data support the ChPT prediction for a cusp in the di-photon invariant mass spectrum at the two pion threshold.

*XXII. International Workshop on Deep-Inelastic Scattering and Related Subjects,*

*28 April - 2 May 2014*

*Warsaw, Poland*

\*Speaker.

†F. Ambrosino, A. Antonelli, G. Anzivino, R. Arcidiacono, W. Baldini, S. Balev, J.R. Batley, M. Behler, S. Bifani, C. Biino, A. Bizzeti, B. Bloch-Devau, G. Bocquet, V. Bolotov, F. Bucci, N. Cabibbo, M. Calveti, N. Cartiglia, A. Ceccucci, P. Cenci, C. Cerri, C. Cheshkov, J.B. Chèze, M. Clemencic, G. Collazuol, F. Costantini, A. Cotta Ramusino, D. Coward, D. Cundy, A. Dabrowski, G. D'Agostini, P. Dalpiaz, C. Damiani, H. Danielsson, M. De Beer, G. Dellacasa, J. Derré, H. Dibon, D. Di Filippo, L. DiLella, N. Doble, V. Duk, J. Engelfried, K. Eppard, V. Falaleev, R. Fantechi, M. Fidecaro, L. Fiorini, M. Fiorini, T. Fonseca Martin, P.L. Frabetti, A. Fucci, S. Gallorini, L. Gatignon, E. Gersabeck, A. Gianoli, S. Giudici, A. Gonidec, E. Goudzovski, S. Goy Lopez, E. Gushchin, B. Hallgren, M. Hita-Hochgesand, M. Holder, P. Hristov, E. Iacopini, E. Imbergamo, M. Jeitler, G. Kalmus, V. Kekelidze, K. Kleinknecht, V. Kozhuharov, W. Kubischta, V. Kurshetsov, G. Lamanna, C. Lazzeroni, M. Lenti, E. Leonardi, L. Litov, D. Madigozhin, A. Maier, I. Mannelli, F. Marchetto, G. Marel, M. Markytan, P. Marouelli, M. Martini, L. Masetti, P. Massarotti, E. Mazzucato, A. Michetti, I. Mikulec, M. Misheva, N. Molokanova, E. Monnier, U. Moosbrugger, C. Morales Morales, M. Moulson, S. Movchan, D.J. Munday, M. Napolitano, A. Nappi, G. Neuhöfer, A. Norton, T. Numao, V. Obraztsov, V. Palladino, M. Patel, M. Pepe, A. Peters, F. Petrucci, M.C. Petrucci, B. Peyaud, R. Piandani, M. Piccini, G. Pierazzini, I. Polenkovich, I. Popov, Yu. Potrebenikov, M. Raggi, B. Renk, F. Retière, P. Riedler, A. Romano, P. Rubin, G. Ruggiero, A. Salamon, G. Saracino, M. Savrié, M. Scarpa, V. Semenov, A. Sergi, M. Serra, M. Shieh, S. Shkarovskiy, M.W. Slater, M. Sozzi, T. Spadaro, S. Stoynev, E. Swallow, M. Szleper, M. Valdata-Nappi, P. Valente, B. Vallage, M. Velasco, M. Veltri, S. Venditti, M. Wache, H. Wahl, A. Walker, R. Wanke, L. Widhalm, A. Winhart, R. Winston, M.D. Wood, S.A. Wotton, O. Yushchenko, A. Zinchenko, M. Ziolkowski.

## 1. Introduction

In 2003-04 the NA48/2 experiment at the CERN SPS used simultaneous  $K^+$  and  $K^-$  beams to collect a large sample of charged kaon decays in the search for direct CP violation [1]. The successor experiment NA62 ( $R_K$  phase) used the same detector with the data-taking conditions optimised for measurement of the ratio,  $R_K$ , of the rates of leptonic kaon decays [2]. The large statistics accumulated by the two experiments have allowed for measurements of a number of rare kaon decay modes, including the radiative  $K^\pm \rightarrow \pi^\pm \gamma\gamma$ .

Experimental studies of radiative non-leptonic decays provide crucial tests for the ability of Chiral Perturbation Theory (ChPT) to describe weak low energy processes. In the ChPT framework, the  $K^\pm \rightarrow \pi^\pm \gamma\gamma$  differential decay rate up to next-to-leading order is parametrised in the following way [3]:

$$\frac{\partial\Gamma}{\partial y \partial x}(\hat{c}, y, z) = \frac{m_K}{2^9 \pi^3} \left[ z^2 (|A(\hat{c}, z, y^2) + B(z)|^2 + |C(z)|) + \left( y^2 - \frac{1}{4} \lambda(1, r_\pi^2, z) \right)^2 |B(z)|^2 \right] \quad (1.1)$$

where  $z = m_{\gamma\gamma}^2/m_K^2$  and  $y = p(q_1 - q_2)/m_K^2$ , and  $p, q_1, q_2$  are the 4-momenta of the kaon and the two photons. The dominant contribution at lowest non-trivial order  $O(p^4)$  comes from the loop term  $A(z, \hat{c})$ , including the pion and kaon loop amplitudes, which depends on an *a priori* unknown  $O(1)$  parameter  $\hat{c}$ . The loop term  $B(z)$  appears only at next-to-leading  $O(p^6)$  order and  $C(z)$  is the pole amplitude. Higher order unitarity corrections from  $K \rightarrow 3\pi$  decays, including the main  $O(p^6)$  contribution as well as those beyond  $O(p^6)$ , have been found to modify significantly the branching ratio and the shape of the  $z$ -spectra. The ChPT predictions for the decay spectra, using the  $O(p^4)$  and  $O(p^6)$  parametrisations with different values of  $\hat{c}$ , are shown in Fig. 1. The di-photon mass spectra exhibit a characteristic cusp at twice the pion mass due to the dominant pion loop amplitude  $A(z)$ . At next-to-leading order there is non-zero differential rate at  $z = 0$  generated by  $B(z)$ . The total branching ratio is predicted to be  $BR(K^\pm \rightarrow \pi^\pm \gamma\gamma) \sim 10^{-6}$ , with the pole amplitude contributing 5% or less [3, 4].

The  $K^\pm \rightarrow \pi^\pm \gamma\gamma$  mode is among the least experimentally studied kaon decays. The only previous measurement [5] has been done by the BNL E787 experiment with 31  $K^+$  candidates in the kinematic region of  $100 \text{ MeV}/c < p_\pi < 180 \text{ MeV}/c$ , where  $p_\pi$  is the pion momentum in the kaon frame. The new NA48/2 [6] and NA62- $R_K$  [7] measurements of the  $K^\pm \rightarrow \pi^\pm \gamma\gamma$  decay at improved precision are reported here.

## 2. Beam line and Detectors

The NA48/2 and its successor NA62- $R_K$  used the same beam line and detector setup but with different beam line parameters and transverse momentum kick of the spectrometer magnet. The two experiments used simultaneous  $K^+$  and  $K^-$  secondary beams with a central momentum of 60 GeV/ $c$  (for NA48/2) and 74 GeV/ $c$  (for NA62- $R_K$ ) derived from the primary 400 GeV/ $c$  proton beam from the SPS impinging on a beryllium target. The beam kaons were delivered to a fiducial decay region contained in a 114 cm long cylindrical vacuum tank. The momenta of the charged decay products were measured in a magnetic spectrometer located downstream of the decay region. The spectrometer consisted of four drift chambers (DCH) and a dipole magnet between the second

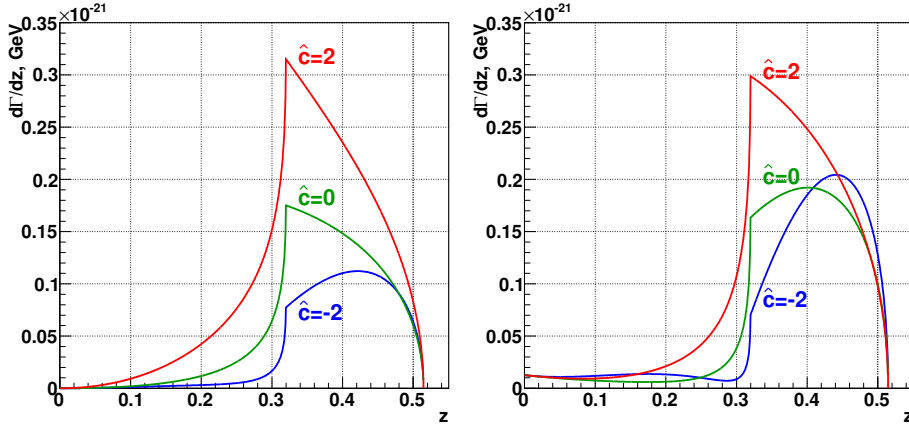


**Figure 1:** ChPT predictions for the differential decay rate in terms of  $z$  for  $O(p^4)$  (left) and  $O(p^6)$  (right) parametrisations with  $\hat{c} = 2; 0; -2$ . The  $O(p^6)$  parametrisation uses values for the  $K \rightarrow 3\pi$  amplitude from a fit to experimental data [9].

and third chambers, which provided a horizontal momentum kick of 120 GeV/c (for NA48/2) and 265 GeV/c (for NA62- $R_K$ ). The nominal spectrometer resolution was  $\sigma_p/p = (1.0 \oplus 0.044.p)\%$  for NA48/2 and  $\sigma_p/p = (0.48 \oplus 0.009.p)\%$  for NA62- $R_K$ , where  $p$  is expressed in GeV/c. The spectrometer was followed by a plastic scintillator hodoscope (HOD), providing fast trigger signals and time measurement of charged particles with a 150 ps resolution. A  $27X_0$  deep liquid Krypton electromagnetic calorimeter (LKr) located further downstream was used for charged particle identification and photon measurement. The LKr active volume of  $7 \text{ m}^3$  was segmented transversely into 13248 projective  $\sim 2 \times 2 \text{ cm}^2$  cells without any longitudinal segmentation. The energy resolution was  $\sigma_E/E = (3.2/\sqrt{E} \oplus 9/E \oplus 0.42)\%$ , and its spatial resolution for the transverse coordinates  $x$  and  $y$  of an isolated electromagnetic shower was  $\sigma_x = \sigma_y = (4.2/\sqrt{E} \oplus 0.6) \text{ mm}$ , where  $E$  is in GeV. A plane of scintillating fibres located at a depth of about  $9.5X_0$  inside the volume of the LKr formed the neutral hodoscope (NHOD) which was used to provide trigger signals. A detailed description of the whole setup, including the detectors not used in this analysis, can be found in [8].

### 3. Event selection

The NA48/2 data come from special minimum bias runs carried out in 2003 and 2004 at  $\sim 10\%$  of the nominal beam intensity. The minimum bias trigger condition was defined as the time coincidence of signals in the same quadrant of both HOD planes and an energy deposit of at least 10 GeV in the LKr. The NA62 data sample was collected in 2007 using several downscaled control trigger chains: i) coincidence of signals in the same quadrant of both HOD planes and a loose lower and upper limits on the DCH hit multiplicity ( $\sim 20\%$  of the sample); ii) condition (i) in coincidence with a LKr energy deposit of at least 10 GeV ( $\sim 60\%$ ); iii) signal in the NHOD ( $\sim 20\%$ ). The  $K^\pm \rightarrow \pi^\pm \gamma\gamma$  decay rate was measured with respect to a normalisation decay chain with a well know branching ratio:  $K^\pm \rightarrow \pi^\pm \pi^0$  followed by  $\pi^0 \rightarrow \gamma\gamma$ . The signal and normalisation data samples were collected simultaneously with the same minimum bias trigger conditions and, as a consequence, the measurement did not depend on the beam flux and composition nor

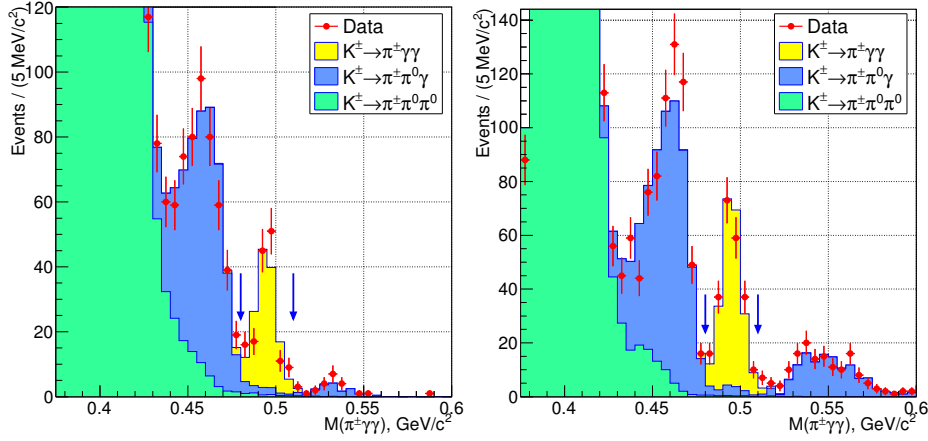


**Figure 2:** The  $\pi^\pm\gamma\gamma$  invariant mass distribution in the NA48/2 (left) and NA62- $R_K$  (right) data samples. The estimated  $K^\pm \rightarrow \pi^\pm\gamma\gamma$  signal corresponds to the result of a ChPT  $O(p^6)$  fit. The  $K^\pm \rightarrow \pi^\pm\pi^0\gamma$  background contributes below, within and above the signal mass region through different mechanisms: photons missing the geometric acceptance (below); merging of photon LKr clusters (within); both, combined with photon conversions in the spectrometer (above). The difference between the left and right plots is due to a different magnetic field in the spectrometer during the NA48/2 and NA62- $R_K$  data-taking. The signal region limits are indicated with vertical arrows.

the trigger downscaling factors and their variation throughout the data taking. Signal events are selected requiring: a  $\pi^\pm$  candidate track, identified by the  $E/p$  ratio of energy deposition in the LKr calorimeter to momentum measured by the spectrometer, which is required to be in the range  $10(8) \text{ GeV}/c < p < 40(50) \text{ GeV}/c$  for the NA48/2 (NA62- $R_K$ ) data; two isolated clusters in the LKr calorimeter separated by at least 25 cm from the track impact point and by at least 20 cm from each other; reconstructed kaon decay vertex located within the fiducial decay region; reconstructed momentum of the  $\pi^\pm\gamma\gamma$  system in agreement with the beam properties; and reconstructed  $\pi^\pm\gamma\gamma$  ( $\pi^\pm\pi^0$ ) invariant mass between 480 and 510  $\text{MeV}/c^2$ . The selection criteria for the signal and normalisation events differ only in the di-photon invariant mass requirement. For  $K^\pm \rightarrow \pi^\pm\gamma\gamma$ , the kinematic region is defined as  $z = (m_{\gamma\gamma}/m_K)^2 > 0.2$  to reject the backgrounds from  $\pi^0$  decays, coming mainly from  $K^\pm \rightarrow \pi^\pm\pi^0$  and peaking at  $z = 0.075$ . For  $K^\pm \rightarrow \pi^\pm\pi^0$ , the di-photon mass is required to be consistent with originating from a  $\pi^0$  decay ( $|m_{\gamma\gamma} - m_{\pi^0}| < 10 \text{ MeV}/c^2$ ).

#### 4. Results and discussion

The  $\pi^\pm\gamma\gamma$  invariant mass distributions from the NA48/2 and NA62- $R_K$  data are shown in Fig. 2, together with the expected signal and background contributions from MC simulations. The NA48/2 signal sample contains 149 candidates with a background contamination of  $15.5 \pm 0.7$  events (232 candidates and  $17.4 \pm 1.1$  events in the NA62- $R_K$  sample). The uncertainties are due to the limited MC statistics. The reconstructed  $z$ -spectra of the candidates as well as the signal and background expectations are shown in Fig. 3. The data confirms the ChPT prediction of a cusp at the two pion threshold.

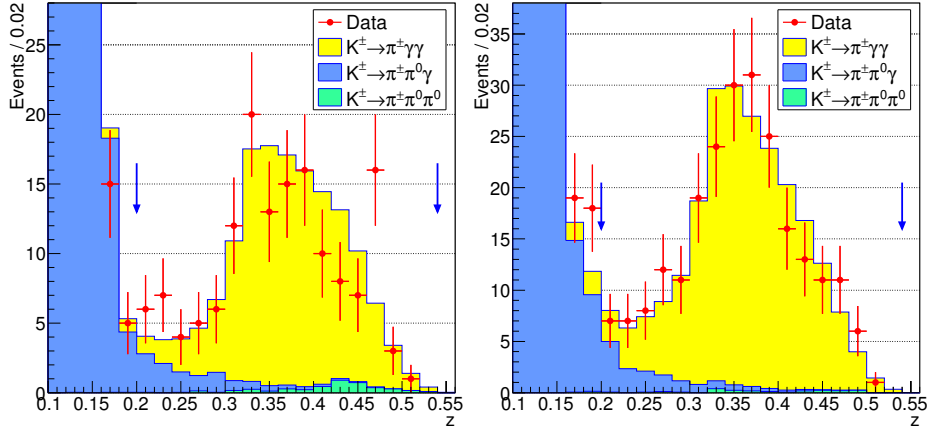


**Figure 3:** Reconstructed  $z = (m_{\gamma\gamma}/m_K)^2$  spectrum of the  $K^\pm \rightarrow \pi^\pm \gamma\gamma$  candidates in the NA48/2 (left) and NA62 (right) data, compared with the estimated contributions from the signal and the largest background  $K^\pm \rightarrow \pi^\pm \pi^0 \gamma$ . The estimated signal is the result of a ChPT  $O(p^6)$  fit. The signal region limits are indicated with vertical arrows.

A model-independent measurement of the partial  $K^\pm \rightarrow \pi^\pm \gamma\gamma$  branching ratios,  $B_j$ , in bins of  $z$  has been performed on the NA48/2 and NA6- $R_K$  data in the kinematic range  $z > 0.2$  (see Fig. 4). Due to the small bin width the dependence of the acceptance on the assumed  $K^\pm \rightarrow \pi^\pm \gamma\gamma$  kinematic distribution can be neglected with respect to the statistical uncertainties. The  $y$ -dependence of the differential decay rate expected within the ChPT framework arises only at next-to-leading order and is weak [3, 4]. The model-independent branching ratio is computed by summing over the  $z$  bins (see Fig. 4), yielding:  $B_{\text{MI}}(z > 0.2) = (0.877 \pm 0.087_{\text{stat}} \pm 0.017_{\text{syst}}) \times 10^{-6}$  for NA48/2 and  $B_{\text{MI}}(z > 0.2) = (1.088 \pm 0.093_{\text{stat}} \pm 0.027_{\text{syst}}) \times 10^{-6}$  for NA62- $R_K$ . The uncertainties are dominated by the statistical ones and the systematics are mainly due to uncertainties of the background estimates.

The  $\hat{c}$  parameter has been measured in the framework of both ChPT  $O(p^4)$  and  $O(p^6)$  parametrisations by performing log-likelihood fits to the reconstructed  $z$ -spectra of the NA48/2 and NA62- $R_K$  data. The  $O(p^6)$  description includes a number of external inputs. There are 7 parameters of the  $K \rightarrow 3\pi$  amplitude which come from a fit to experimental data [9], and three polynomial terms  $\eta_i$  ( $i = 1, 2, 3$ ) which have been set to  $\eta_j = 0$ . Both  $O(p^4)$  and  $O(p^6)$  descriptions involve the parameter  $G_8$  which is fixed in this study according to Ref. [10]. The values of the  $\hat{c}$  parameter obtained from the fits are presented in Table 1. Using the  $\hat{c}_6$  values in the ChPT parametrisation, the model-dependent  $K^\pm \rightarrow \pi^\pm \gamma\gamma$  branching ratios have been estimated by integrating the  $O(p^6)$  differential decay rate over the whole physical region of the kinematic variables (Table 1).

The NA48/2 and NA62- $R_K$  measurements of the model-independent ratio and the  $\hat{c}_6$  parameter have been combined. The systematic uncertainties on the combined results have been estimated by studying their stability with respect to variation of the selection conditions applied separately to the independent NA48/2 and NA62- $R_K$  data samples. The branching ratio in the full kinematic range considering the combined value of the  $\hat{c}_6$  parameter in the parametrisation is  $B_{\text{ChPT}} = (1.003 \pm 0.051_{\text{stat}} \pm 0.024_{\text{syst}}) \times 10^{-6}$ . The branching fraction measured by the BNL

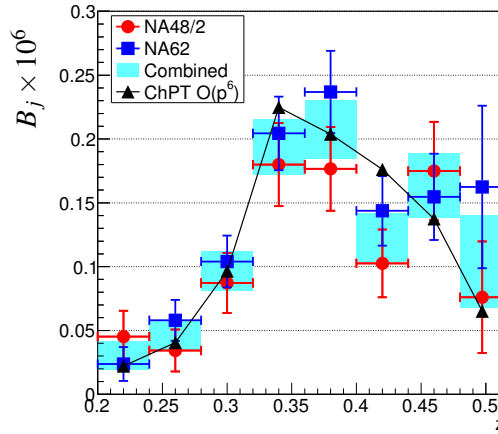


**Figure 4:** Measurement of the model-independent branching ratios in  $z$  bins by NA48/2 and NA62, and the combination of the two. The values of  $B_j$  computed within ChPT  $O(p^6)$  formulation are obtained by integration of the ChPT differential decay rate for the central value of the combined measurement  $\hat{c} = 1.86$  over the bin width.

	$\hat{c}_4$	$\hat{c}_6$	$B_{\text{ChPT}}(\hat{c}_6)$
NA48/2	$1.37 \pm 0.33_{\text{stat}} \pm 0.14_{\text{syst}}$	$1.41 \pm 0.38_{\text{stat}} \pm 0.11_{\text{syst}}$	$(0.910 \pm 0.072_{\text{stat}} \pm 0.022_{\text{syst}}) \times 10^{-6}$
NA62- $R_K$	$1.93 \pm 0.26_{\text{stat}} \pm 0.08_{\text{syst}}$	$2.10 \pm 0.28_{\text{stat}} \pm 0.18_{\text{syst}}$	$(1.058 \pm 0.066_{\text{stat}} \pm 0.044_{\text{syst}}) \times 10^{-6}$
Combined	$1.72 \pm 0.20_{\text{stat}} \pm 0.06_{\text{syst}}$	$1.86 \pm 0.23_{\text{stat}} \pm 0.11_{\text{syst}}$	$(1.003 \pm 0.051_{\text{stat}} \pm 0.024_{\text{syst}}) \times 10^{-6}$

**Table 1:** Results for the ChPT  $\hat{c}$  parameter from fits to the  $z$ -distribution of  $K^\pm \rightarrow \pi^\pm \gamma\gamma$  decays and the model-dependent branching ratios obtained using the ChPT  $O(p^6)$  description.

E737 [5] is  $(1.10 \pm 0.32) \times 10^{-6}$  and the parameter  $\hat{c}$  is  $1.6 \pm 0.6$  at  $O(p^4)$  and  $1.8 \pm 0.6$  at  $O(p^6)$ . The new results from the NA48/2 and NA62- $R_K$  measurement of the  $K^\pm \rightarrow \pi^\pm \gamma\gamma$  decay agree with earlier data and improve significantly on the previous experimental precision.

## References

- [1] J.R. Batley *et al.*, Eur. Phys. J **C52** (2007) 875.
- [2] C. Lazzeroni *et al.*, Phys. Lett. **B719** (2013) 326.
- [3] G. D’Ambrosio and J. Portolés, Phys. Lett. **B386** (1996) 403.
- [4] J.-M. Gérard, C. Smith and S. Trine, Nucl. Phys. **B730** (2005) 1.
- [5] P. Kitching *et al.*, Phys. Rev. Lett. **79** (1997) 4079.
- [6] J.R. Batley *et al.*, Phys. Lett. **B730** (2014) 141.
- [7] C. Lazzeroni *et al.*, Phys. Lett. **B732** (2014) 65.
- [8] V. Fanti *et al.*, Nucl. Instrum. Methods **A574** (2007) 433.
- [9] J. Bijnens, P. Dhonte and F. Persson, Nucl. Phys. **B648** (2003) 317.
- [10] V. Cirigliano *et al.*, Rev. Mod. Phys. **84** (2012) 399.